Surface Review and Letters, Vol. 29, No. 9 (2022) 2250120 (20 pages)

DOI: 10.1142/S0218625X22501207

World Scientific
www.worldscientific.com

MODELING AND OPTIMIZING THE TENSILE BEHAVIOR OF DEVELOPED ALUMINUM HYBRID COMPOSITE

OLANREWAJU S. ADESINA*,§, ADEOLU A. ADEDIRAN†, ABAYOMI A. AKINWANDE‡, OLUYEMI O. DARAMOLA‡ and OLUFEMI O. SANYAOLU*

*Department of Mechanical Engineering, Redeemer's University, Ede, Osun–State, Nigeria

†Department of Mechanical Engineering, Landmark University, Kwara State, Nigeria

‡Department of Metallurgical and Materials Engineering, Federal University of Technology, Akure, Nigeria

§osaadesina@yahoo.com; abypublications@gmail.com

Received 31 January 2022
Revised 26 May 2022
Accepted 19 June 2022
Published 5 August 2022

Aluminum and its alloy are versatile metal materials engaged in various applications based on their high strength, corrosion resistance and light weight. However, there are many limitations to its applications when compared with steel. In a bid to improve on the properties, aluminum composites are developed. In this study, Al 6111 composite was developed by the blend of silica and bamboo leaf ash (BLA) as reinforcement employing stir casting process. The input factors for the experiment were silica dosage (A), BLA proportion (B) and stirring temperature (C). The experimental design was carried out via Box Behnken design of the response surface methodology. Composites were fabricated through stir casting process by varying the inputs according to the dictations of the experimental runs. Parameters evaluated are yield strength, ultimate tensile strength, elastic modulus and elongation. Result of the ANOVA analysis showed that the parameters had consequential effect on the response and the developed model for each parameter are fit for predictions. From the surface plot, interaction between 5 wt.% and 10 wt.% silica and 2 wt.% and 4 wt.% BLA led to improvement in yield, ultimate tensile strength but decrease in elongation even as proportions 10 wt.% and 15 wt.% silica and 4 wt.% and 6 wt.% BLA ensued reduction in the value. Stirring temperature of 700–800°C is favorable to the strength parameters while 800–900°C led to strength reduction. Optimization via response surface, predicted optimum conditions of 11.6249 wt.%, 3.95707 wt.% and 789.033°C for A, B and C, respectively. Predicted values for yield strength, ultimate tensile strength, elastic modulus and elongation are 278.26 MPa, 378.24 MPa, 97.7885 GPa and 10.132%, respectively. Validation experiment was carried out at the optimum condition and the deviation in parameters between the predicted and validated values is $< 5\%$. Hence, the models are statistically fit for property predictions.

Keywords: Al 6111; bamboo leaf ash; Box-Behnken design; optimization; silica; stirring temperature.

§Corresponding author.

1. Introduction

Demand for aluminum alloys and their composites keep rising with tine on account of the versatility afforded by the materials. Aluminum alloys have found applications in aerospace, marine, automobile and industries owing to the high strength to specific weight. For the purpose of employing aluminum as replacement of steel, several attempts have been made for the improvement of aluminum matrix with additives resulting in aluminum composites. Varying studies involved in production of Aluminum matrix composites (AMC) engaged the use of reinforcements in the matrix. The reinforcement can be in form of particulate, whiskers or fibers.[1] Particle reinforcement are classified into synthesized and agro-based type. The reinforcements are majorly ceramic-based particulates like silica, alumina, titania, boron carbide, silicon carbide, silicon nitride, tungsten carbide and aluminum nitride, which are of the synthetic origin.[2–5] Agro-based are ashes of coconut shell, rice husk, bamboo leave, egg shell and snail shell. Industrial-based waste like fly ash and waste glass have also found application in reinforcing aluminum matrix.[6] In addition to that, particles of copper, titanium and nickel have also been involved in the processing of AMCs. Hybrid aluminum composites involve combination of two or more of these particulates as reinforcements. According to Surappa,[7] advantages of AMCs over the base matrix are better strength, enhanced stiffness, lower density, enhanced high temperature performance, better wear resistance and high damping performance. The points highlighted are corroborated by the review of Bodurin *et al.* and Sharma *et al.*[8,9]

Different production methods are involved in the development of AMCs which include stir casting, friction stir processing, squeeze casting, spray codeposition, liquid infiltration, reactive process and sintering.[10–13] Stir casting is commonly employed owing to its low processing cost, simplicity and ability for mass production.[14] This process entails employment of particle reinforcement in aluminum melt involving mechanical stirring. The act of stirring allows the particulate to be dispersed within the melt. Parameters considered in stir casting include stirring temperature, speed, time, particulate preheating temperature, blade angle, size of the stirrer, position of the stirrer and powder feed rate.[15,16] These properties determine the microstructure and properties of the developed composite.

Silica is a common reinforcement for aluminum composite development that has been investigated with consequent effect in enhancing properties of the developed composite as reported by Singh *et al.*[17] in which hardness and wear resistance were improved with particulate loading. In the investigations carried out by Thirumalvalavan and Senthilkumar,[18] improvement of ultimate tensile strength, yield strength, hardness and impact strength when aluminum matrix was reinforced with silica particles was reported. Optimum performance for all properties was recorded at 8 wt.% silica. Thirumalai *et al.*[19] reinforced Al LM 9 with SiO_2 at 3, 4.5, 6 and 9 wt.%. Tensile strength improved progressively as the proportion increased from 3 wt.% to 9 wt.%. Same experience was noted for hardness and wear resistance. Silica was concluded to be a good reinforcement for aluminum alloys.

On the other hand, a series of investigations have been done employing agro-based ash as reinforcement. Bamboo leaf ash (BLA) for instance has been investigated. Alaneme and Adewuyi[20] observed enhancement fracture toughness of the composite with BLA addition. A comparable study carried out by Atuanya *et al.*[21] prepared Al-Si-Mg/BLA composites adding the ash at 5, 10 and 15 wt.%. The outcome of the study showed that tensile strength and hardness were improved with the proportion of the bamboo ash particles. Similarly, Baburja *et al.*[22] observed improvement of yield and ultimate strengths of Al 6061 composite developed. Silica and BLA can be said to play an important role in enhancing properties of developed composite.

Onto producing hybrid composite, few studies had considered the blend of silica and BLA in the fabrication of AMC. In developing countries, silica is imported, hence, it is of high cost. BLA is cheaper to obtain since its available in abundance within the environment. Towards supplementing silica use as reinforcement, this study considered BLA as supplement in Al 6111 composite development for the purpose of lowering cost of procuring silica as reinforcement agent. Moreso, few studies had considered optimization of the process towards achieving optimal condition for the blend of silica and BLA in AL 6111 composite. In this study, silica and BLA were utilized as reinforcement in the fabrication of Al

Table 1. Levels of factors in the design of experiment.

Factors	Low level (wt.%)	Medium level (wt.%)	High level (wt.%)
Silica dosage (A)	5	10	15
BLA (B)	2	4	6
Stirring temperature (C)	700	800	900

6111 hybrid composites for various engineering application. Stir casting was adopted for the process on account of the cost effectiveness and simplicity. However, the process is often accompanied by porosity, agglomeration of particles blow holes and segregation. According to Ref. 5, optimization of stir casting processing parameters is a way to go in minimizing the existence of defects in stir cast sample. To that effect, this study focused on optimization of casting parameters involving silica dosage, BLA proportion and stirring temperature. Mechanical property focused on by the study are tensile properties entailing yield strength, ultimate tensile strength, elastic modulus and elongation. Box-Behnken design was involved in the experimental design. Experimental factors are silica dosage (A) chosen in the range of 5–15 wt.% following the study of Hamouda *et al.*[23]; bamboo leave ash (BLA) proportion (B) in the range of 2–6 adopted after the study of Ref. 24 and stirring temperature (C).

2. Materials and Methods

2.1. *Design of experiment by Box–Behnken method*

Box–Behnken design (BBD) is a design of experiment method meant to investigate parameters with reduced experimental runs. It is a rotatable second-order-three-level-factorial design of the cube form which made of the central points, middle points and the edge point.[25] In this investigation, input factors are proportion of silica dosage (A), BLA proportion (B) and stirring temperature (C). In BBD, number of experimental trails is estimated with the equation $N = 2k(K - 1) + C$. N stands for number of experimental trials, K stands for number of factors and C stands for number of central points. According to Wang *et al.*,[26] Box-Behnken is preferred to other response surface design hence adopted in this study. Seventeen runs (17) of experiment were lined out for each of the response parameter (Table 2).

2.2. *Material preparation, composite development and tensile test*

Bamboo leaves were collected, washed with distilled water and allowed to dry in the open for 8 h. The dried leaves were calcined in a muffle furnace at 800°C for 8 h and allowed to cool to room temperature. Lump ash was broken into powder and the ash was sieved to $-45\,\mu$m and employed for composite development. High purity silica powder was employed for the composite preparation. Silica and BLA were mixed according to the mix design provided in Table 2 after which they were preheated to 500°C before introduction into the melt. Procured aluminum 6111 ingot was melted in a preheated graphite crucible (preheated to 500°C). The melt was stirred at 500 rpm for 15 min as effected in Ref. 5 before introducing preheated reinforcement into the melt according to the dictation of the experimental runs (Table 2). Stir casting temperature, dosage of silica and proportion of BLA were varied in accordance to the experimental runs (Table 2) obtained via BBD approach.

The tensile properties of the composites produced were evaluated by tensile testing using an Instron universal testing machine (ISTRON 3369) (Table 1). As shown in Figs. 1(a) and 1(b), samples were machined to dimensions length of 120 mm, gauge length of 60 mm and gauge diameter of 10 mm in line with ASTM, E8/E8M-21.[27] The specimens were mounted on the testing platform and pulled monotonically at a strain rate of 10^{-3}/s until fracture. The tests were performed at room temperature following recommendations of ASTM, E8/E8M-21.[27] For each composite composition, three repeat tensile tests were performed to guarantee the reliability of the data generated. Parameters deduced from obtained results were yield strength, ultimate tensile strength, elastic modulus and elongation. Microstructural characterization was affected utilizing scanning electron microscope (Philips/FEI XL 30S FEG-SEM). The surface of the samples was initially grinded with grades of grinding paper after which the surface was polished to a mirror like surface. Etching was done on the surface by application of 0.5% hydrogen fluoride

Table 2. Experimental runs, coded level and responses.

	Coded levels			Factors			Responses			
Experimental runs	A	B	C	A (wt.%)	B (wt.%)	C (°C)	YS	UTS	EM	El
1	0	−1	−1	5	4	700	187.5	322.3	79.5	16.1
2	0	0	0	10	6	900	143.7	261.6	62.3	8.3
3	1	1	0	5	6	800	186.9	305.7	68.8	11.7
4	−1	0	−1	10	2	900	163.9	282.4	71.3	11.7
5	0	−1	1	5	4	900	149.4	288.1	70.5	12.6
6	0	0	0	10	4	800	283.8	384.6	91.7	10.8
7	−1	1	0	10	4	800	289.5	387.6	95.9	10.6
8	0	1	1	10	2	700	228.8	316.8	80.3	15.4
9	−1	0	1	15	4	900	128.1	269.6	90.4	8.2
10	1	0	1	10	4	800	285.7	375.6	96.2	10.3
11	1	−1	0	15	6	800	157.7	281	87.8	7.6
12	0	1	−1	15	2	800	180	306.9	99.3	10.9
13	1	0	−1	10	6	700	200.1	292.5	70.4	10.5
14	−1	−1	0	10	4	800	284.9	389.6	90.7	11
15	0	0	0	5	2	800	213.8	329.1	78.5	17.1
16	0	−1	−1	10	4	800	288.4	388.6	94.3	10.9
17	0	0	0	15	4	700	175	301.4	101.2	10

Notes: A is silica dosage, B is BLA proportion, C is stirring temperature, YS is the yield strength (MPa), UTS is the ultimate tensile strength (MPa), EM is elastic modulus (GPa), El is elongation (%).

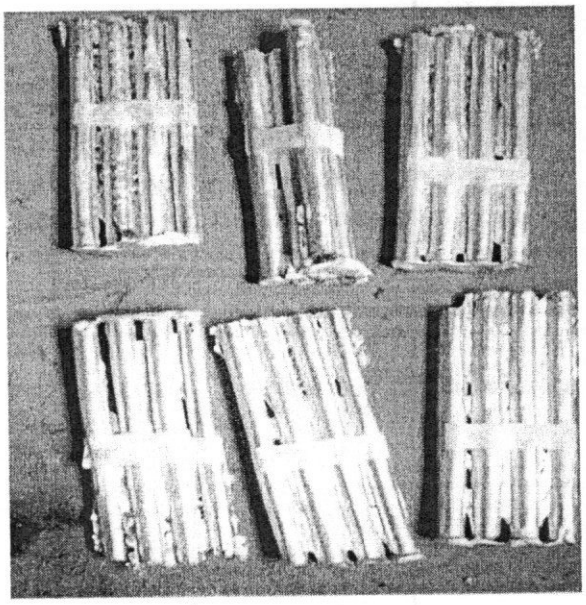

(a)

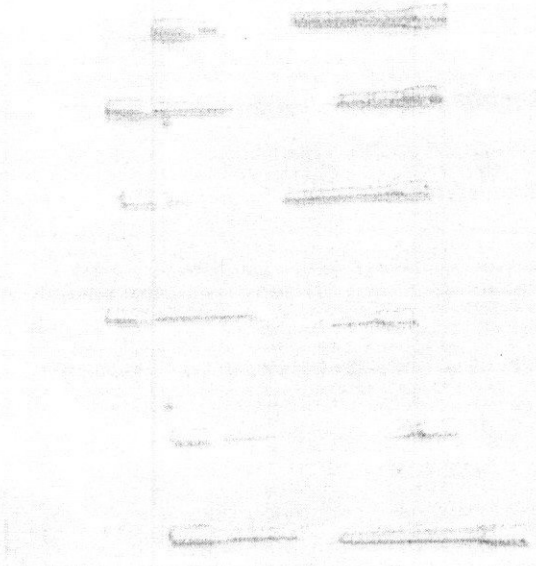

(b)

Fig. 1. (a) and (b) As-cast aluminum-based composites produced for machining of tensile test specimens.

solution for 20 s via swabbing. Sequel to this is the rinsing with distilled water dried using a laboratory drier before subjecting to microstructural test.

3. Results and Discussion

3.1. *ANOVA for Quadratic model*

Response 1: Yield strength of the developed composite

ANOVA of yield strength of the developed composite is highlighted in Table 3. Input variables SiO_2, bamboo leaf fiber and stirring temperature shared significant contribution on yield strength response of the composite ($p < 0.05$). Cross-interactions AB, AC and BC are insignificant, of which interactions A^2, B^2 and C^2 are significant going by the p-value being < 0.05. As presented in the table, the model is significant based on the p-value which is < 0.05. This depicts that the model represents the data and can be employed in the prediction of the response. The lack-of-fit which depicts the deviation between the model and the residual is insignificant confirming that the model is statistically fit. Coefficient of correlation R^2 is 0.9944 showing that the model is a good relation between the model and the residuals. R^2 (adj) is 0.9872 while R^2 (pred) is 0.9166, the difference between the two is < 0.2, further validating the model as statistically fit.

$$\begin{aligned} YS = &-3834.475 + 51.034A + 61.95375B + 9.89843C \\ &+ 0.115AB + 0.0044AC + 0.010625BC \\ &- 2.5197AA - 9.71688BB - 0.006347CC \end{aligned} \quad (1)$$

Equation (1) represents the model; YS is the yield strength response. In the model, it is indicated that parameters A, B and C have positive coefficient. This depicts the fact that SiO_2, bamboo leaf fiber and stirring temperature has positive resultant or synergetic effect on yield strength output, likewise interactions AB and AC. On the other hand, interactions BC, AA, BB and CC are antagonistic to the response.

Figure 2(a) is the probability plot for the residuals as per yield strength. The experimental data are expressed along the line-of-fit depicting no outliner further indicating that the model is statistically fit to represent the data. Figure 2(b), on the other hand, represents the data plotted randomly around the horizontal zero line. This satisfied the concept of constant variance, further affirming the fitness of the model.

Response 2 Ultimate tensile strength

ANOVA result, as it affects ultimate tensile strength of the composites, is illustrated in Table 4. The contributions of the input variables; SiO_2 dosage, bamboo leaf fiber proportion and stirring temperature on ultimate tensile strengths are portrayed to be significant going by their p-values being < 0.05, whereas,

Table 3. Analysis of variance on yield strength of the developed composite.

Source	Sum of squares	df	Mean square	F-value	p-value	
Model	52,195.69	9	5799.52	137.90	< 0.0001	significant
A-SiO_2	1171.28	1	1171.28	27.85	0.0012	
B-BLA	1202.95	1	1202.95	28.60	0.0011	
C-ST	5319.96	1	5319.96	126.50	< 0.0001	
AB	5.29	1	5.29	0.1258	0.7333	
AC	19.36	1	19.36	0.4603	0.5193	
BC	18.06	1	18.06	0.4295	0.5332	
A^2	16,707.60	1	16,707.60	397.27	< 0.0001	
B^2	6360.77	1	6360.77	151.24	< 0.0001	
C^2	16,960.52	1	16,960.52	403.28	< 0.0001	
Residual	294.39	7	42.06			
Lack of Fit	271.30	3	90.43	15.67	0.1112	insignificant
Pure Error	23.09	4	5.77			
Cor Total	52,490.08	16				
$R^2 = 0.9944$			$R^2(\text{adj}) = 0.9872$		$R^2(\text{pred}) = 0.9166$	

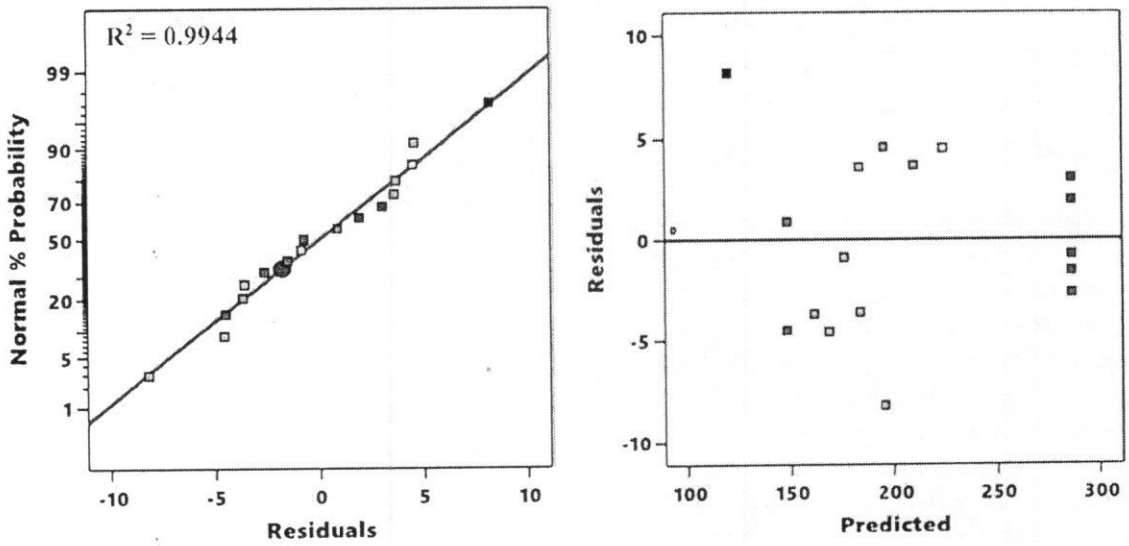

Fig. 2. Diagnostic plots for yield strength (a) normal probability plot (b) residuals vs predicted plot.

cross interactions AB, AC, BC have insignificant influence on the response. Interactions A^2, B^2, C^2 demonstrated significant influence on the response ($p < 0.05$). The model expressed in Eq. (2) is significantly confirmed by the lack-of-fit which p-value to > 0.05 as it should be for a fit model. Going by the coefficient of correlation R^2 which is 0.9758, the model is said to have a good correlation with the residuals. Going by the value of adjusted R^2 (0.9703) and predicted R^2 (0.9166), the difference between the two is < 0.2, thereby affirming the model to be statistically fit in predicting the response.

$$\begin{aligned}\text{UTS} = {} & -3165.725 + 26.1325\text{A} + 77.775\text{B} + 8.38238\text{C} \\ & - 0.0625\text{AB} + 0.0012\text{AC} + 0.004375\text{BC} \\ & - 1.45\text{AA} - 10.81875\text{BB} - 0.005360\text{CC} \quad (2)\end{aligned}$$

Equation (2) expressed the model for prediction of ultimate tensile strength. As revealed by the model, experimental factors A, B and C have positive coefficient; hence, SiO_2, bamboo leaf fiber and stirring temperature as experimental inputs are synergetic to the response; ditto, interactions AC and BC.

Table 4. Analysis of variance on ultimate tensile strength.

Source	Sum of Squares	*df*	Mean Square	*F*-value	*p*-value	
Model	32,614.84	9	3623.87	183.16	< 0.0001	significant
A-SiO_2	930.96	1	930.96	47.05	0.0002	
B-BLA	1113.92	1	1113.92	56.30	0.0001	
C-ST	2154.96	1	2154.96	108.92	< 0.0001	
AB	1.56	1	1.56	0.0790	0.7868	
AC	1.44	1	1.44	0.0728	0.7951	
BC	3.06	1	3.06	0.1548	0.7057	
A^2	5532.89	1	5532.89	279.65	< 0.0001	
B^2	7885.16	1	7885.16	398.54	< 0.0001	
C^2	12,096.67	1	12,096.67	611.40	< 0.0001	
Residual	138.50	7	19.79			
Lack of Fit	9.30	3	3.10	0.0959	0.9583	not significant
Pure Error	129.20	4	32.30			
Cor Total	32,753.34	16				
$R^2 = 0.9758$			$R^2(\text{adj}) = 0.9703$		$R^2(\text{pred}) = 0.9693$	

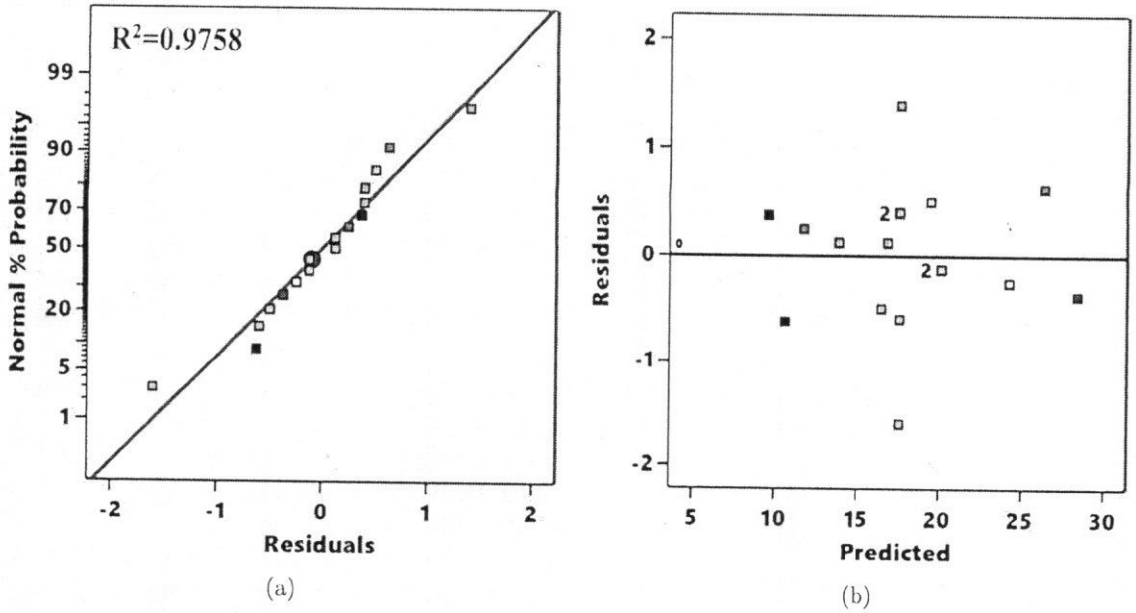

Fig. 3. Diagnostic plots for ultimate tensile strength (a) normal probability plot (b) residuals vs predicted plot.

Interactions AB, AA, BB and CC are referred to as the negative terms of the model, hence, antagonistic to the response.

Figure 3(a) presents the probability plot for water absorption response, the residuals are aligned along the normal line, depicting the residual is normally distributed along the mean response. As detected in Fig. 3(b), the plots are randomly scattered; hence, the assumption of constant variance is satisfied.

Response 3 Elastic modulus of the developed composite

ANOVA of elastic modulus is as showcased in Table 5. The input factors which are silica dosage, bamboo fiber proportion and stirring temperature have p-values < 0.05; therefore, they have significant contribution on the parameter. Interactions AB, AC, BC and A^2 are realized to be insignificant while interaction B^2 and C^2 have significant influence on the

Table 5. Analysis of variance on elastic modulus.

Source	Sum of squares	df	Mean square	F-value	p-value	
Model	2354.19	9	261.58	69.33	< 0.0001	significant
A-SiC	828.24	1	828.24	219.53	< 0.0001	
B-BLA	201.00	1	201.00	53.28	0.0002	
C-ST	170.20	1	170.20	45.11	0.0003	
AB	0.8100	1	0.8100	0.2147	0.6572	
AC	0.8100	1	0.8100	0.2147	0.6572	
BC	0.2025	1	0.2025	0.0537	0.8234	
A^2	18.26	1	18.26	4.84	0.0637	
B^2	631.07	1	631.07	167.27	< 0.0001	
C^2	459.14	1	459.14	121.70	< 0.0001	
Residual	26.41	7	3.77			
Lack-of-Fit	1.98	3	0.6592	0.1079	0.9511	not significant
Pure Error	24.43	4	6.11			
Cor Total	2380.60	16				
$R^2 = 0.9789$			$R^2(\text{adj}) = 0.9649$		$R^2(\text{pred}) = 0.9607$	

response. The model represented in Eq. (3) is statistically significant, affirmed by the lack-of-fit which is insignificant. Coefficient of correlation for the model is $R^2 = 0.9789$; it therefore means the residuals has very small variance or deviation from the model. Coefficient of correlation R^2 is 0.9789 indicating there is a strong relationship between the model and the residuals (since value is > 0.95). R^2 (adj) is 0.9649 while R^2 (pred) is 0.9607 and since the difference between the two R^2 values is < 0.2, the model is affirmed to be fit for prediction of elastic modulus.

$$\begin{aligned} \mathrm{EM} = & -594.025 + 1.269\mathrm{A} + 21.52875\mathrm{B} + 1.62918\mathrm{C} \\ & - 0.045\mathrm{AB} - 0.0009\mathrm{AC} + 0.001125\mathrm{BC} \\ & + 0.0833\mathrm{AA} - 3.06063\mathrm{BB} - 0.001044\mathrm{CC} \quad (3) \end{aligned}$$

The expression for the model is presented in Eq. (3), where EM is the elastic modulus. As noted in the model, SiO_2 dosage, BLA proportion and stirring temperature are favorable to elastic modulus having synergetic effect on the response. This goes for interactions BC and AA. Conversely, interactions AB, AC, BB and CC are not favorable exhibiting antagonist effect on the response.

Figure 4(a) presents the probability plot for elastic modulus from which it is noted that the residuals are expressed along the normal line. In essence, it is interpreted that the data is normally distributed along the fit. In Fig. 4(b), since the plots are randomly scattered along the "0" line, then, the data are accepted to have no correlation.

Response 4 Elongation

ANOVA of elongation of the composite under tensile load is depicted in Table 3. Input variables SiO_2, bamboo leaf fiber and stirring temperature shared significant contribution on yield strength response of the composite ($p < 0.05$). Also, all interactions had significant effect of elongation of the composite going by the p-value being < 0.05. As demonstrated in the table, the model is significant based on the p-value which is < 0.05. This depicts that the model [Eq. (4)] represents the data and can be employed in the prediction of the response. The lack-of-fit which depicts the deviation between the model and the residual is insignificant further affirming a statistically fit model. Coefficient of correlation R^2 is 0.9688 affirming the model there is a good relationship between the model and the residuals. R^2 (adj) is 0.9823 while R^2 (pred) is 0.9757, the difference between the two is < 0.2; validating the model as statistically fit with regards to elongation.

$$\begin{aligned} \mathrm{El} = & 71.65 - 1.925\mathrm{A} - 3.9425\mathrm{B} - 0.0824\mathrm{C} \\ & + 0.0525\mathrm{AB} + 0.00085\mathrm{AC} + 0.001875\mathrm{BC} \\ & + 0.0271\mathrm{AA} + 0.106875\mathrm{BB} + 0.000033\mathrm{CC} \quad (4) \end{aligned}$$

El is the elongation, A, B and C are SiO_2 dosage, bamboo fiber proportion and stirring temperature, respectively. In the model, it is indicated that parameters A, B and C have negative coefficient. This depicts the fact that SiO_2, bamboo leaf fiber and stirring temperature have negative resultant or

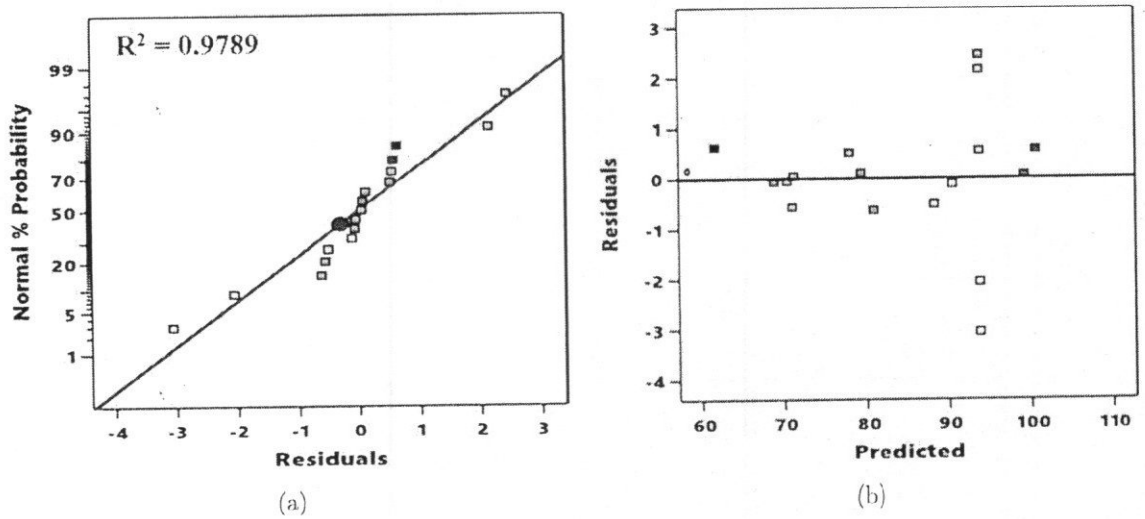

Fig. 4. Diagnostic plots for compressive strength (a) normal probability plot (b) residuals vs predicted plot.

Table 6. Analysis of variance on elongation.

Source	Sum of squares	*df*	Mean square	*F*-value	*p*-value	
Model	111.75	9	12.42	229.94	< 0.0001	significant
A-SiC	54.08	1	54.08	1001.48	< 0.0001	
B-BLA	36.13	1	36.13	668.98	< 0.0001	
C-ST	15.68	1	15.68	290.37	< 0.0001	
AB	1.10	1	1.10	20.42	0.0027	
AC	0.7225	1	0.7225	13.38	0.0081	
BC	0.5625	1	0.5625	10.42	0.0145	
A^2	1.93	1	1.93	35.79	0.0006	
B^2	0.7695	1	0.7695	14.25	0.0069	
C^2	0.4516	1	0.4516	8.36	0.0233	
Residual	0.3780	7	0.0540			
Lack of Fit	0.0700	3	0.0233	0.3030	0.8229	not significant
Pure Error	0.3080	4	0.0770			
Cor Total	112.13	16				
$R^2 = 0.9866$			$R^2(\text{adj}) = 0.9823$		$R^2(\text{pred}) = 0.9757$	

antagonistic effect on elongation. On the other hand, parameters AB, AC, BC, AA, BB and CC are synergetic to the response (Table 6).

Figure 5(a) presents the probability plot for elongation of which the residuals are aligned along the normal line 0, except for an outliner. This outlines a point; the residual is normally distributed along the mean response. As observed in Fig. 5(b), the plots are randomly scattered, hence the assumption of constant variance is satisfied and no correlation between the values.

3.2. *Response surface and contour plots*

Response surface plot presents manner of the interplay between the factors and their effect on the response. Meanwhile, the contour plot exhibits varying region of the response diverse factor combinations.

3.2.1. *Yield strength*

Figure 6 reveals the surface plot (6a) and contour plot (6b) for yield strength. Interaction between silica and bamboo fiber ash and the effect on yield strength at

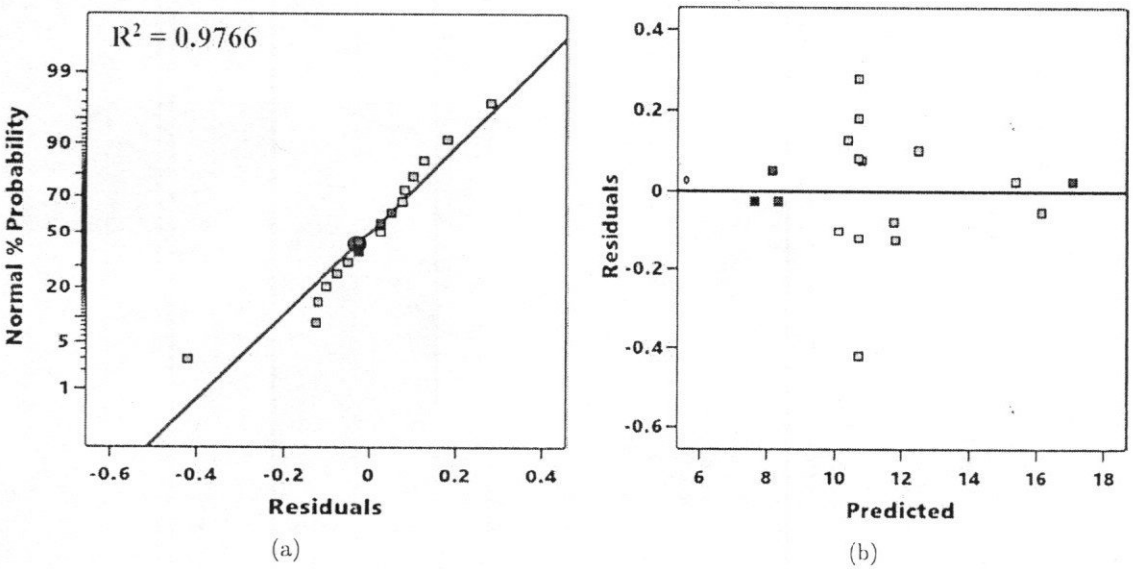

Fig. 5. Diagnostic plots for elongation (a) normal probability plot (b) residuals vs predicted plot.

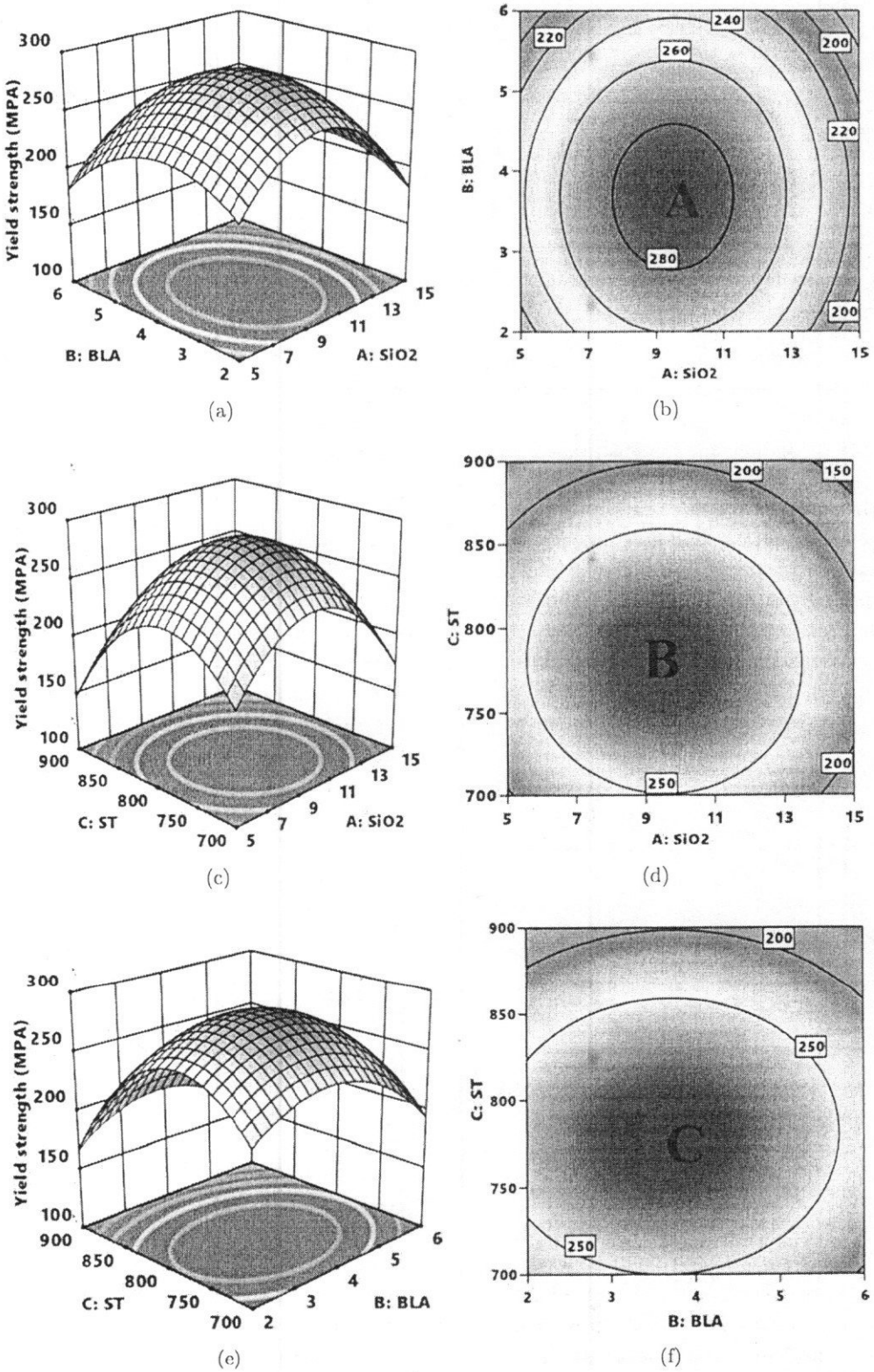

Fig. 6. Response surface and contour plots revealing effects of interactions on yield strength as represented by interactions (a, b) SiO_2 vs BLA (c, d) SiO2 vs stirring temperature (e, f) BLA vs stirring temperature.

SiO2 is silica dosage, BLA is bamboo leave ash proportion, ST is stirring temperature.

constant 800°C is highlighted in Fig. 6(a). The collage of 5–10 wt.% SiO_2 and 2–4 wt.% bamboo leave fiber ash engendered strength enhancement. Beyond such proportion, that is combination of 10–15 wt.% SiO_2 and 4–6 wt.% BLA, there was strength reduction. The rise in strength is attributed to the dispersion of the particles within the matrix permitting even stress distribution. A similar result is replicated in Ref. 21 in which progressive enhancement in tensile strength of Al-Si-Mg alloy was effected by addition of BLA. The reduction in strength on addition of 10–15 wt.% BLA and 4–6 wt.% SiO_2 is on account of coagulation of the particles yielding points of stress concentration consequent of which result is reduction in strength.[28] Region tagged A in Fig. 6(b) is the optimum region in which optimal tensile strength 280–300 MPa can be attained for yield strength when combining 7.6–11.4 wt.% SiO_2 and 2.8–6.6 wt.% BLA when temperature is held at 800°C.

The amity between silica and stirring temperature, holding BLA at 4 wt.% is exhibited in Fig. 6(c). SiO_2 dose of 5–10 wt.% infused into the mix between 700°C and 800°C at constant BLA proportion of 4 wt.% ensued improvement in yield strength on account of even dispersion of the particles whereas, 10–14 wt.% SiO_2 combination with constant 4 wt.% BLA at temperature range of 800–900°C resulted in depreciation in strength. A similar observation was reported by Alaneme and Adewuyi[20] in which tensile strength reduced with the infusion of the blend of alumina and BLA in Al-Mg-Si. Enhancement in strength between 700°C and 800°C is associated with moderate temperature for dispersion of particles within the melt. The portion tagged B in the contour plot presented in Fig. 6(d) is the optimum zone for yield strength when combining SiO_2 in the range of 5–15 wt.% and 4 wt.% constant proportion of BLA employing temperature range of 700–900°C. From the plot, it is deduced that yield strength of 250–270 MPa can be realized when combining silica between 2.4 wt.% and 13.3 wt.% with BLA 4 wt.% at temperature range of 700–840°C.

Figure 6(e) highlights the influence of the interactive pattern between BLA and stirring temperature when silica is held constant at 10 wt.%. 2–4 wt.% BLA infusion into the melt between temperature range of 700–800°C results in enhancement effect of the yield strength; meanwhile, BLA proportion of 4–6 wt.% inclusion at temperature range of 800–900°C spawned strength decrease. The decrease in strength between 800°C and 900°C is based on the effect of high temperature reaction amounting to formation of intermetallic which are detrimental to strength of the alloy. Portion labeled C in the contour plot of Fig. 6(f) is the region in which maximum strength value of 250–300 MPa when combining 2–5.6 wt.% BLA with 10 wt.% silica at temperature range of 700–860°C.

3.2.2. *Ultimate tensile strength*

Figure 7 highlights the surface plot of the interactivity between the input factors and the effect on the response (ultimate tensile strength). As observed, the blend of 5–10 wt.% silica and 2–4 wt.% BLA in the melt at constant temperature of 800°C kindled enhancement of the response. The feat is related with the ability of the particles to fill in pores within the matrix, thereby reducing interparticle distance, outcome of which amounted to strength enhancement. Akinwande *et al.*[28] associated the feat to the mechanism of solution strengthening in which the particles served as inhibitors to the easy mobility of dislocation. Thirumalvalavan and Senthilkumar[29] experienced similar outcomes when silica was introduced into Al LM 25. It was noted that ultimate strength improved between 0 wt.% and 8 wt.%, while decrement in strength was revealed between 8 wt.% and 12 wt.% silica. Similar outcome was reported by Ogunsanya *et al.*[30] with TiO_2 reinforcement of Al 6061. On the other hand, the collage of 10–15 wt.% silica and 4–6 wt.% BLA at 800°C spawned reduction in the strength response. The contour plot showcased in Fig. 7(b) depict zone C as the optimum region in which strength value of 380–400 MPa UTS value is attainable when the blend of 7.2–11.2 wt.% silica and 3.4–4.5 wt.% BLA holding stirring temperature at 800°C.

Figure 7(c) depicts the surface plot of the interaction between silica and temperature on ultimate strength, holding BLA constant at 4 wt.%. Silica dosage of 5–10 wt.% and 4 wt.% constant BLA at temperature range of 700–800°C exhibited increasing ultimate tensile strength. Conversely, input of 10–15 wt.% silica and stirring temperature of 800–900°C have negative influence on the response value resulting in depreciation in strength. Temperature between 700°C and 800°C facilitated even dispersion of the particles within the melt on account of moderate

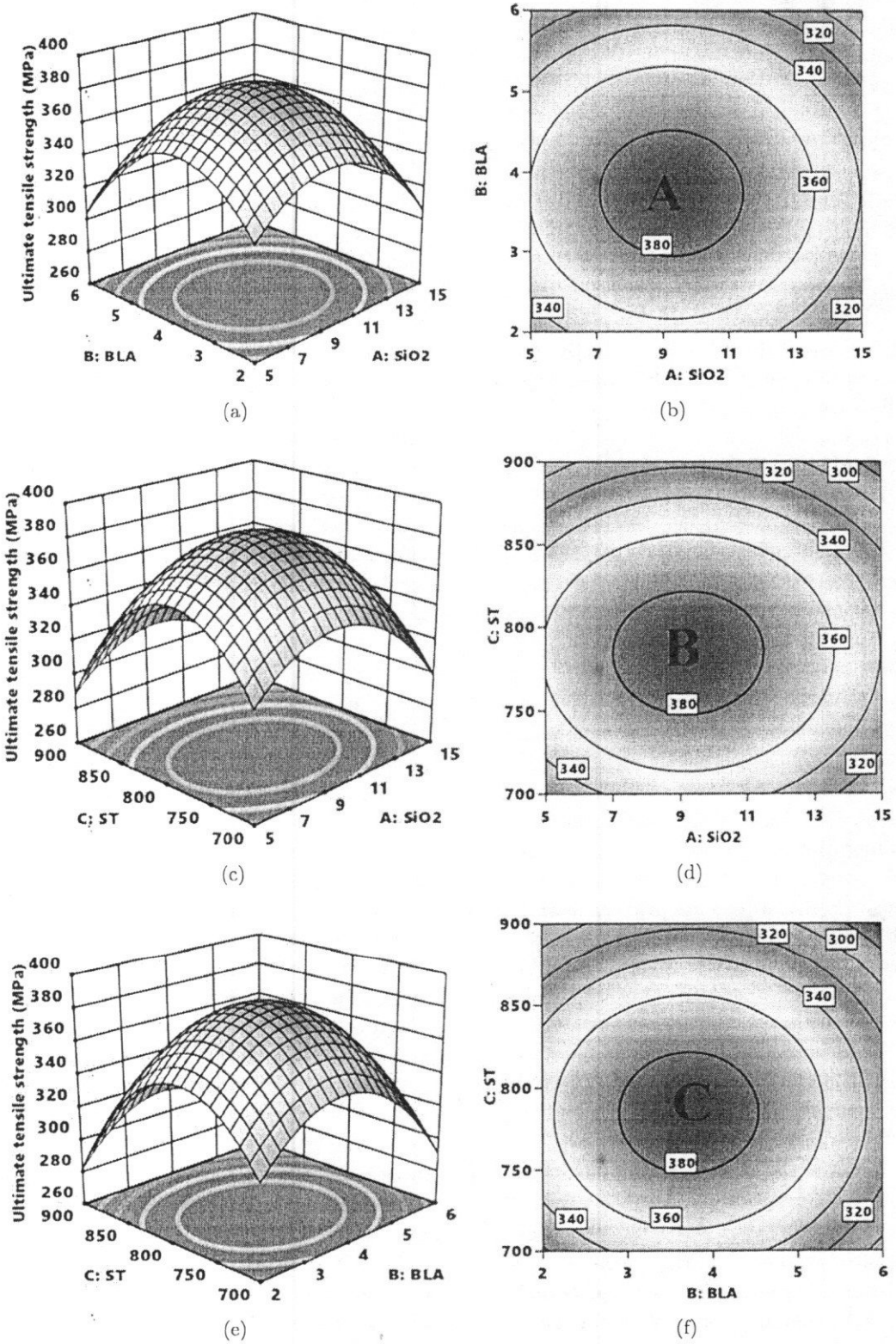

Fig. 7. Response surface and contour plots revealing effects of interactions on ultimate tensile strength as represented by interactions (a, b) SiO2 vs BLA (c, d) SiO2 vs stirring temperature (e, f) BLA vs stirring temperature.

SiO2 is silica dosage, BLA is bamboo leave ash proportion, ST is stirring temperature.

viscosity of the melt. However, temperature between 800°C and 900°C is high enough for high viscosity in the melt. The outcome of such led to absorption of gas and air and during solidification, the air and gas content are forced to be evolved. As a result, there exist pores and blowholes significance of which lower resistance to deformation under loading. The decrease in strength between 10 wt.% and 15 wt.% silica can occur on account of higher particle density of the particles leading to easy particle-matrix debonding.[28] As regards to the influence of the particles on strength, Mallikarjuna and Basavaraj[31] experienced improvement in strength with a peak at 9 wt.% on incorporation of silica and reduction in strength at 12 wt.%. Figure 7(d) shows the contour plot portraying the optimum region labeled as B. Strength value of 380–400 MPa is realizable when 7.1–8.2 wt.% silica is blended with 4 wt.% fixed BLA employing stirring temperature in the range of 760–825°C.

Figure 7(e) demonstrates the surface plot of the interplay existing between BLA and stirring temperature when fixing silica constant at 10 wt.%. 2–4 wt.% BLA and 10 wt.% fixed silica utilized as reinforcing particles in the melt between 700°C and 800°C ensure strength enhancement. The feat occurs on the dint of strong adhesion between the particles and the matrix and enhanced particle strengthening serving as obstacle to transversing of dislocation within the matrix. However, 4–6 wt.% with 10 wt.% fixed silica at stirring temperature of 800–900°C impact negatively on the strength performance. The observation is related to agglomeration of the particles. Temperature also played a role in the reduction in strength in the sense that existence of inetrmetallics at high temperature lowers strength of the composites. Figure 7(f) reveals diverse regions in which varying responses are obtained at diverse factor combination. The optimum zone labeled C ranged between 380 MPa and 400 MPa for the response. Varying in the input value is 2.9–4.6 wt.% BLA and 760–824°C temperature at 10 wt.% constant silica dosages.

3.2.3. *Elastic modulus*

Figure 8 showcases the surface plot and contour plot for elastic modulus response. Figure 8(a) presents the result of the interaction between silica and bamboo fiber ash on elastic modulus when temperature is held constant at 800°C. The immix of 5–15 wt. % SiO_2 and 2–4 wt.% bamboo leave fiber ash spawned increase in modulus. Nonetheless, combination of 5–15 wt.% SiO_2 and 4–6 wt.% BLA at 800°C stirring temperature amounted to decrease in modulus. Increase in modulus is based on reduced interparticle distance and lower porosity which enhanced the stiffness of the composite. The reduction is traceable to the brittle nature of the particulates. Silica is brittle, hence at certain percentage in the mix, the brittle nature played a role amounting to reduction in modulus. Region tagged A in Fig. 8(b) is the optimum region in which optimal elastic modulus of 100–120 GPa is attainable when input factors are varied; 13–15 wt.% SiO_2 and 2.2–4.7 wt.% BLA.

Amity between silica and stirring temperature as it affects elastic modulus when holding BLA constant at 4 wt.% is exhibited in Fig. 8(c). SiO_2 dose of 5–15 wt. % inclusion with 4 wt.% BLA at constant proportion of 4 wt.% and stirring temperature range of 700–800°CC provoked improvement in elastic modulus whereas, 5–15 wt.% SiO_2 combination with constant 4 wt.% BLA at temperature range of 800–900°C resulted in depreciation in the modulus. Anand *et al.*[32] had explained the role of particulate inclusion on elastic modulus. The role of the reduction in the stiffness is based on the presence of voids and blow holes at that temperature. The defects under loading easily allow propagation of crack. The portion tagged B in the contour plot presented in Fig. 8(d) is the optimum zone for elastic modulus when combining SiO_2 in the range of 5–15 wt.% and 4 wt.% constant proportion of BLA, employing temperature range of 700–900°C. From the plot, it is deduced that elastic modulus of 100–120 GPa can be attained when blending silica between 13 wt.% and 15 wt.% with fixed BLA 4 wt.% at temperature range of 700–830°C.

Figure 8(e) highlights the influence of the interactive pattern between BLA and stirring temperature when silica is held constant at 10 wt.% on elastic modulus. 2–4 wt.% BLA addition into the melt between temperature range of 700–800 % has enhancement effect of the modulus; meanwhile, BLA proportion of 4–6 wt.% inclusion at temperature range of 800–900°C triggered strength depreciation. Portion labeled C in the contour plot of Fig. 8(f) is the region in which maximum modulus value of 90–100 GPa for such combination is attained. The input

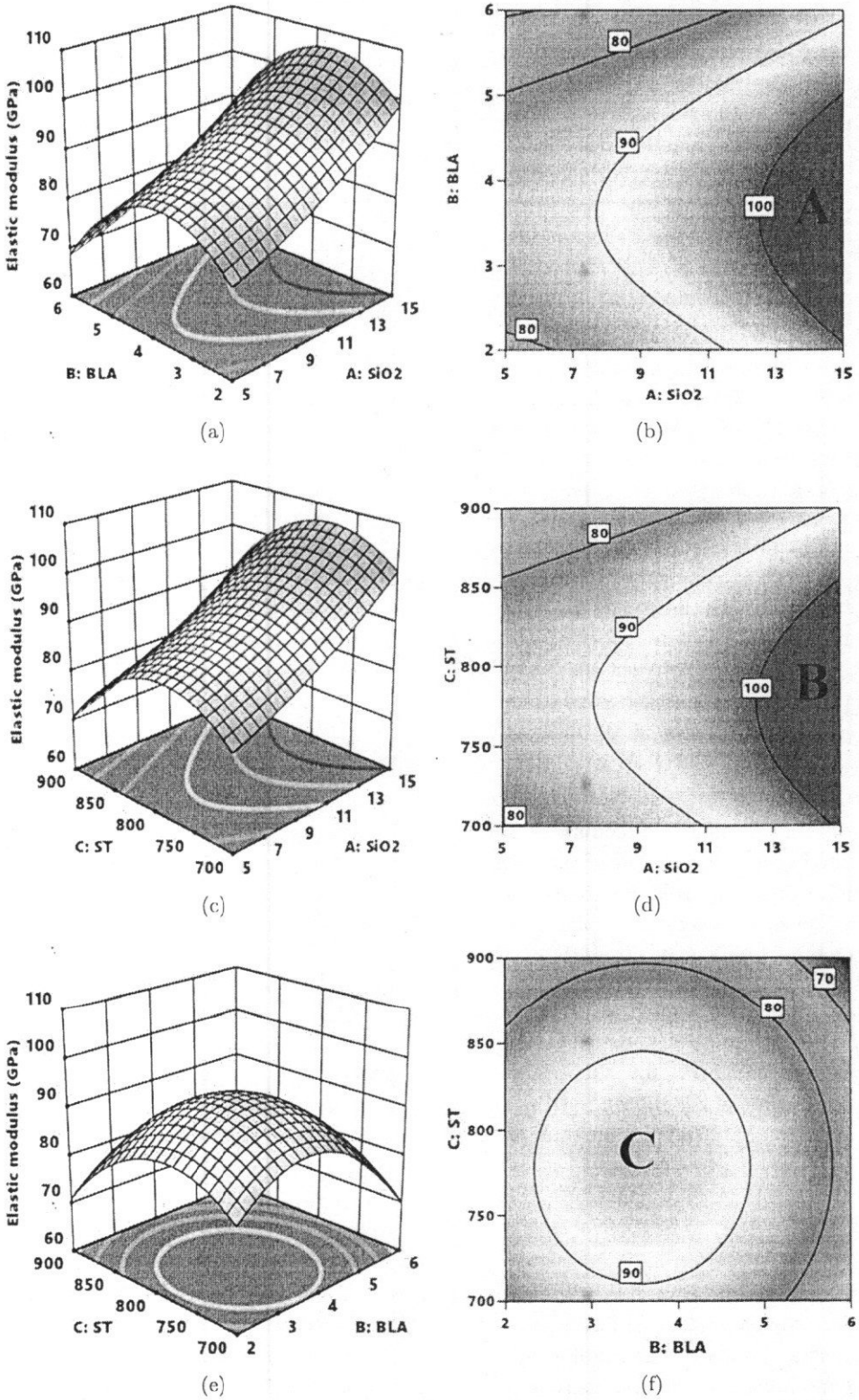

Fig. 8. Response surface and contour plots revealing effects of interactions on elastic modulus as represented by interactions (a, b) SiO_2 vs BLA (c, d) SiO_2 vs stirring temperature (e, f) BLA vs stirring temperature.

SiO2 is silica dosage, BLA is bamboo leave ash proportion, ST is stirring temperature.

range for the optimum modulus is 2–5.6 wt.% BLA with 10 wt.% silica at temperature range of 700–860°C.

3.2.4. *Elongation*

Figure 9(a) demonstrates the surface plot of the interaction which occurred between the input factors and the effect on elongation of the composite. The collage of 5–15 wt.% silica and 2–6 wt.% BLA in aluminum matrix at constant temperature of 800°C stimulated reduction in elongation. Similar feat was observed with Bannaravuri and Birru[33] in which progressive inclusion of BLA provoked decrease in elongation. The decrease in elongation in this study is imputable to enhanced stiffness with increasing particle content. Figure 9(b) depicts zone A as the optimum region in which elongation value of 8–6% is attainable blending 13.6–15 wt.% silica and 5.2–6.0 wt.% BLA holding stirring temperature at 800°C.

Figure 9(c) depicts the surface plot of the interaction between silica and temperature on ultimate strength, holding BLA constant at 4 wt.%. Silica dosage of 5–15 wt.% and 4 wt.% constant BLA at temperature range of 700–900°C ensued reduction in elongation. Uniformly dispersed particles in matrix play a role in inhibiting dislocation movement, consequently reducing elongation. This is aided by moderate temperature which permits even dispersion of particles based on moderate viscosity of the melt. Outcome of the ceramic particulate reinforcement in Swamy *et al.*[34] is in consistence with the result presented in this study as progressive particulate reinforcement triggered decrease in elongation. Figure 9(d) shows the contour plot depicting the optimum region labeled as B. Elongation of 10–8% is attainable when 10–15 wt.% silica is blended with 4 wt.% fixed BLA employing stirring temperature in the range of 710–900°C.

Figure 9(e) demonstrates the surface plot of the interplay existing between BLA and stirring temperature when fixing silica constant at 10 wt.%. Proportions between 2 wt.% and 6 wt.% BLA and 10 wt.% fixed silica employed in the melt between 700°C and 900°C amounted in decrease in elongation. Sivakumar *et al.*[35] had reported reduction in elongation with rise in particulate reinforcement, an observation which is in tandem with the findings of this study. Figure 9(f) reveals diverse regions in which varying responses are obtained at diverse factor combination. The optimum region is tagged C in which elongation value of 10–8% is realizable. Varying in the input value is 3.8–6 wt.% BLA and 725–900°C temperature at 10 wt.% constant silica dosages.

3.3. *Microstructural analysis*

Figures 10(a) and 10(b) are the samples prepared at 700°C and as observed there are particulate coagulation which is one of the features of lower stirring temperature. When the temperature is low, the viscosity is low which promotes coagulation and separation within the melt. These are points of stress concentration within the composite reflecting lower strength performance. Figures 10(c) and 10(d) are samples produced at 800°C in which dispersion of particles is observed. At moderate temperature, there is enough viscosity which permits the particles to be dispersed within the matrix. This is in consonance with observations reported in Ref. 5. Disperse particles lowers porosity and interparticle distance which permit distribution of stress evenly within the matrix. Also, dispersed particles serve as obstacle preventing free navigation of dislocation. One distinct feature of particle strengthening is increase in dislocation density around the particles effect of which result in strengthening of the material. Figures 10(e) and 10(f) represent particles prepared at high temperature of 900°C. At high temperature, there are tendency for gas entrapment, inclusions and chemical reactions which results in formation of intermetallic phases as observed in the Figs. 10(e) and 10(f). Therefore, different conditions produce different features at the microstructural level producing varying performance on the material.

XRD analysis

Figure 11 features the phase identification for selected samples prepared at 700°C, 800°C and 900°C. Figure 10(a) indicates the phase indentation for sample cast at 700°C. Identified phases are Al, Fe and SiO_2. The SiO_2 is based on the presence of silica and BLA present in the microstructure. At 800°C [Fig. 11(b)], silica content is observed to increase associated with moderate casting temperature which allowed even dispersion of the particles within the melt as indicated in Figs. 10(c) and 10(d). This supported strength

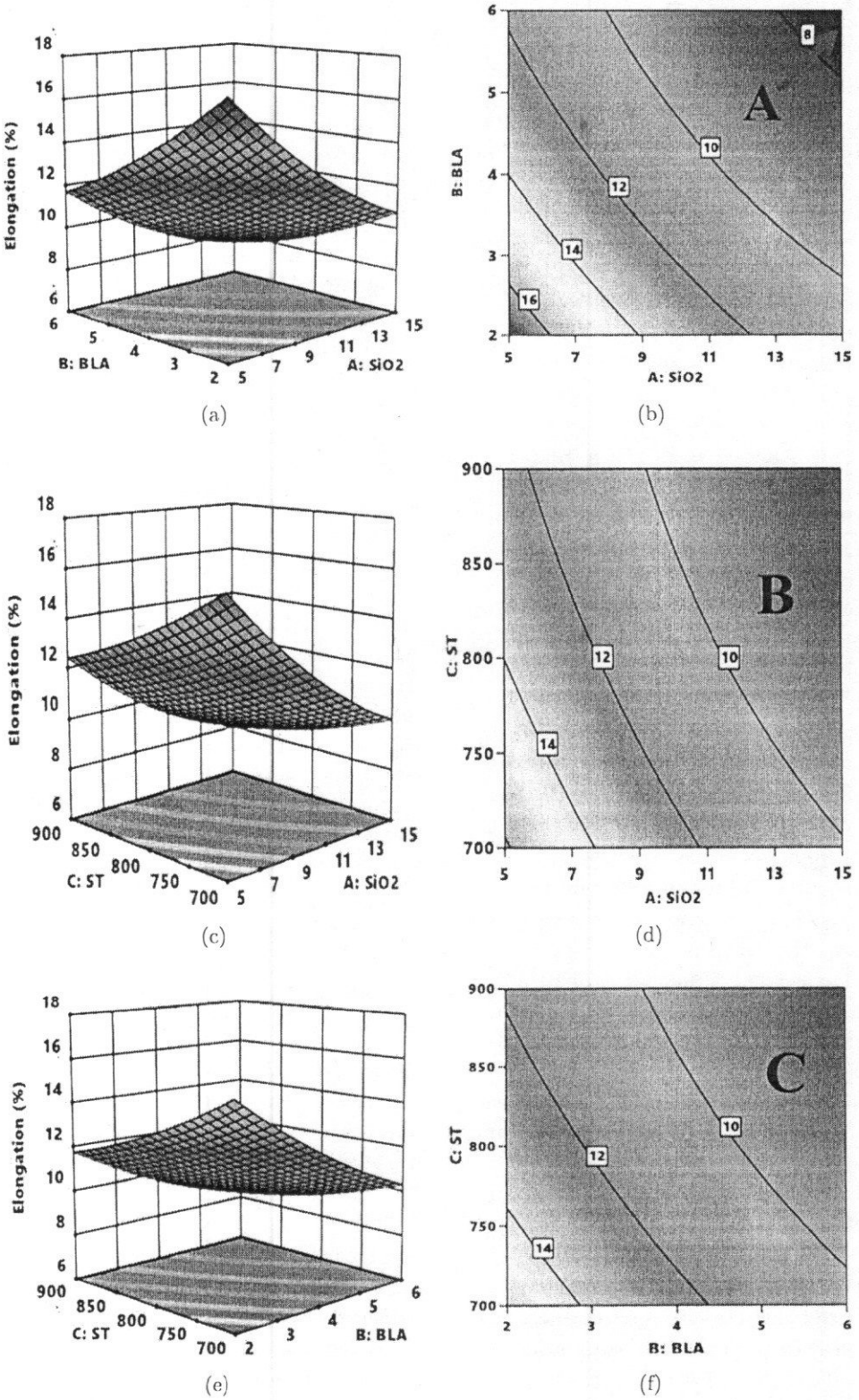

(a) (b) (c) (d) (e) (f)

Fig. 9. Response surface and contour plots revealing effects of interactions on elongation as represented by interactions (a, b) SiO_2 vs BLA (c, d) SiO_2 vs stirring temperature (e, f) BLA vs stirring temperature.

SiO2 is silica dosage, BLA is bamboo leave ash proportion, ST is stirring temperature.

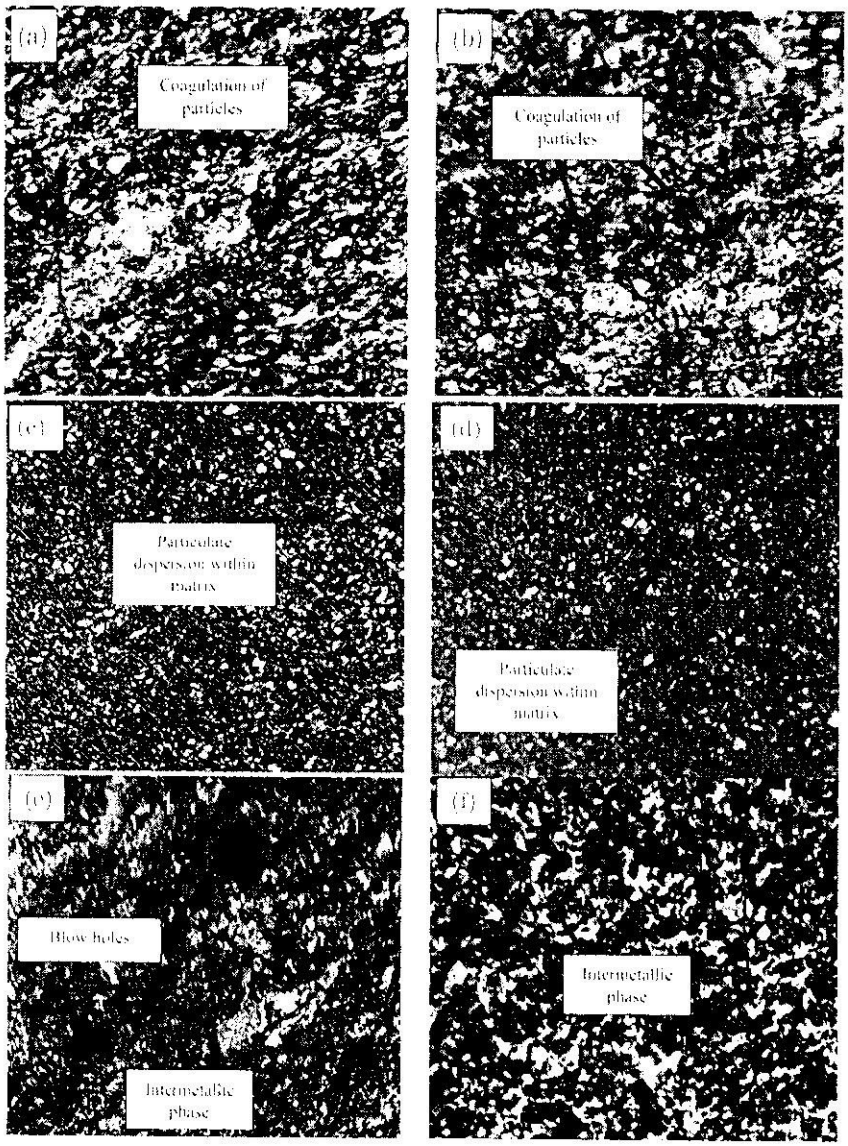

Fig. 10. (a)–(f) present the micrograph of composite samples prepared at different conditions.

improvement in the composite yielding better performance as compared with the sample prepared at 700°. Figure 11(c) indicates the phases present in samples cast at 900°C. the phases showed presence of Al, Fe and SiO_2 associated with elemental with the particulate addition. Intermetallic phases such as $MgZn_2$, Al_5FeSi and Al_6FeMn are also identified. These phases occur as a result of high temperature reaction with the present elements in the melt. These phases are identified to be deleterious to strength and ductility, a reason for the lower performance of samples at high temperature compared with strength performance at 800°C.[36,37]

3.4. *Optimization and results validation procedure*

Constraints

Response surface methodology was utilized for optimization of the investigated parameters employing design expert 13. The constraints for the optimization are stated in Table 7 and the result of optimization presented in Fig. 10. Optimum parameter obtained from the optimization are 11.6243 wt.%, 3.95849 wt.% and 789.119°C were for silica dosage, BLA and stirring temperature, respectively. Predicted values for yield and ultimate tensile strength,

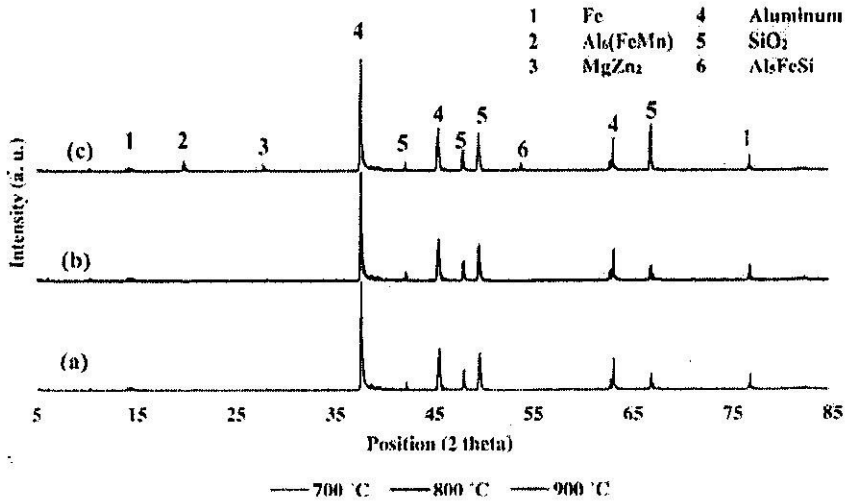

Fig. 11. Phase identification.

Table 7. Optimization criteria.

Name	Goal	Lower Limit	Upper Limit	Lower Weight	Upper Weight	Importance
A: SiO_2	is in range	5	15	1	1	3
B: BLA	is in range	2	6	1	1	3
C:ST	is in range	700	900	1	1	3
YS	maximize	128.1	289.5	1	1	3
UTS	maximize	261.6	389.6	1	1	3
EM	maximize	62.3	101.2	1	1	3
El	minimize	7.6	17.1	1	1	3

elastic modulus and elongation are presented in Table 8.

Validation experiment was carried out with the optimal nix in which case ~11.62 wt.% SiO_2 and ~3.96 wt.% BLA were combined as reinforcement as temperature of ~789.12°C. Four samples were tested for each property and the values realized for yield and ultimate tensile strength, elastic modulus and elongation are showcased in the table. From the error obtained for each property which is < 5%, it is affirmed that the models are statistically fit in the r\prediction of the responses.

As observed in Table 8, for each of the properties error is < 5%, hence, can be deduced that the models are validated to be statistically fit.

Table 8. Predicted values vs experimental values.

Properties	Predicted values	Experimental values	% Error
Yield strength	278.248 MPa	284.6 MPa	2.28
Ultimate tensile strength	379.232 MPa	359.9 MPa	4.83
Elastic modulus	97.7817 GPa	98.96 GPa	1.21
Elongation	10.1296 %	9.7 %	4.20

4. Conclusion

Aluminum AA 6111 composite was prepared by stir casting process by the incorporation of silica BLA. Process factors were varied as silica dosage (A), BLA proportion (B) and stirring temperature (C). The following conclusions arrived at;

(a) the result of the analysis of variance showed that the variable factors had significant influence on the parameters. Also, the models obtained for the responses were satisfied to be fit for prediction of the responses.

(b) surface plots presented for each property parameter showed that the response of the parameters depended on the interactive behavior between the parameters. Equally, the contour plot revealed the optimum zone for each parameter and varying ranges where the optimum can be achieved.

(c) optimum condition as obtained from the optimization prediction is 11.6249 wt.%, 3.95707 wt.% and 789.033°C for silica dosage, bamboo leave fiber and stirring temperature, respectively. Predicted values for the parameters are 278.26 MPa, 378.24 MPa, 97.7885 GPa and 10.132% for yield strength, ultimate tensile strength, elastic modulus and elongation, respectively. Meanwhile, validation experiment was carried out at the optimum conditions and values obtained for each of the parameters are 284.6 MPa, 359.9 MPa, 98.96 GPa and 9.7%, respectively. When compared with the predicted values, the error obtained for each parameter is $< 5\%$ affirming the models to be competent in predicting the responses.

(d) microstructural features showed that at temperature of 700°C, particulate coagulation was observed. At 800°C, the particulates were observed to be dispersed within the matrix. At temperatures of 900°C, intermetallic phases and blow holes are observed. These features were indicated to affect the property performance of the composite.

Acknowledgments

This paper is supported by the Department of Mechanical Engineering, the Redeemer's University, Ede, Nigeria and Department of Metallurgical and Materials Engineering, the Federal University of Technology, Nigeria.

Funding

The authors received no funding from any source.

Competing Interest

The authors declare no competing interest with any previous work.

Data Availability

All data employed in support to the outcome of the study are included in this article.

References

1. M. P. Behera, T. Dougherty and S. Singamneni, *Procedia Manuf.* **30** (2019) 159. https://doi.org/10.1016/j.promfg.2019.02.023.
2. S. Debnath and A. K. Pramanick, *Ethics Inf. Technol.* **2** (2020) 147. https://doi.org/10.26480/etit.02.2020.147.150.
3. K. Shirvanimoghaddam, H. Khayyam, H. Abdizadeh, M. K. Akbarim, A. H. Pakseresht, E. Ghasali and M. Naebe, *Mater. Sci. Eng.A* **658** (2016) 135. https://doi.org/10.1016/j.msea.2016.01.114.
4. K. Ravikumar, K. Kiran and V. S. Sreebalaji, *Measurement* **102** (2017) 142. https://doi.org/10.1016/j.measurement.2017.01.045.
5. A. A. Adediran, A. A. Akinwande, O. A. Balogun, B. J. Olorunfemi and M. Saravana Kumar, *Sci. Rep.* **11** (2021) 19860. https://doi.org/10.1038/s41598-021-99168-1.
6. A. A. Adediran, A. A. Akinwande, O. A. Balogun, O. S. Adesina, A. Olayanju and T. Mojisola, *Sci. Afr.* (2021). https://doi.org/10.1016/j.sciaf.2021.e00812.
7. M. K. Surappa, *Sadhana* **28** (2003) 319.
8. M. O. Bodunrin, K. K. Alaneme and L. H. Chown, *Mater. Res. Technol.* **4** (2015) 434.
9. R. Sharma, P. J. Saurabh, K. Kakkar, K. Kamboj and P. Sharma, *Int. Res. J. Eng. Technol.* **4** (2017) 832.
10. G. F. Ayna'em, *Adv. Mater. Sci. Eng.* **2020** (2020) 1. https://doi.org/10.1155/2020/3765791.
11. M. Ravikumar, H. N. Reddappa and R. Suresh, *Mater. Today Proc.* **5** (2018) 23796. https://doi.org/10.1016/2020/3765791.
12. P. Raghuvaran, M. Suresh, S. Aakash, M. Balaji, K. D. Kumar and S. H. Prasath, *IOP Conf. Ser. Mater. Sci. Eng.* **995** (2020) 012040. https://doi.org/10.1088/1757-899X/995/1/012040.
13. T. R. Vijayaram and V. P. M. Baskaralal, *Int. J. Eng. Res. Technol.* **9** (2016) 45.
14. B. Suresh and N. S. V. Moorthi, *rocedia Eng.* **64** (2013) 1183. https://doi.org/10.1016/Jj.proeng.2013.09.197.
15. M. O. Durowoju, J. O. Agunsoye, L. O. Mudashiru, A. A. Yekinni, S. K. Bello and T. O. Rabiu, *Eur. J. Eng. Res. Sci.* **2** (2017) 5. https://doi.org/10.24018/ejers.2017.2.11.498.
16. K. Ahmadhoni and S. Khan, *J. Mech. Civil Eng.* **12** (2015) 22. https://doi.org/10.9790/1684-126442240.
17. M. Singh, K. Goyal and D. K. Goyal, *Univ. J. Mech. Eng.* **3** (2015) 142.
18. S. Thirumalvalavan and N. Senthilkumar, *Int. J. Eng. Mater. Sci.* **26** (2019) 59.
19. T. Thirumalai, L. Boopathi and T. Shreedhar, *Int. Conf. Emerging Trends in Engineering, Science and Sustainability Technology* (2017), pp. 30–36.
20. K. K. Alaneme and E. O. Adewuyi, *Assoc. Metall. Eng. Serbia* **19** (2013) 177.
21. C. C. Atuanya, A. T. Esione and F. A. Anene, *J. Chin. Adv. Mater. Soc.* (2018). https://doi.org/10.1080/22243682.2018.1722276.

22. K. Baburaja, D. S. C. Kishore, S. R. T. Rasari, V. S. Alusuri, M. J. Shaik, A. Lingineni and R. Ravuri, *International Journal of Mechanical Engineering and Technology* **8** (2017) 344.
23. A. M. S. Hamouda, S. Sulaiman, T. R. Vijayaram, M. Sayuti and M. H. M. Ahmad, *Journal of Achievements of Materials and Manufacturing Engineering* **25** (2007) 11.
24. K. T. Shridhara, S. Hanumnthlal and T. M. R. Annoji, *Int. J. Eng. Res. Technol.* **4** (2015) 446.
25. S. L. C. Ferreira, R. E. Bruns, H. S. Ferreira, G. D. Matos, J. M. David, G. C. Brandao, E. G. P. Da Silva, L. A. Portugal, P. S. Dos Reis, A. S. Souza and W. N. L. Dos Santos, *Anal. Chim. Acta* **597** (2007) 179. https://doi.org/10.1016/j.aca.2007.07.011.
26. C. N. Wang, N. A. T. Nguyen and T. T. Dang, *Appl. Sci.* **10** (2020) 1. https://doi.org/10.3390/app10248959.
27. ASTM E 8/E8M-21, ASTM International, West Conshohocken, PA (2021).
28. A. A. Akinwande, O. A. Balogun and V. Romanovski, *Environ. Sci. Pollut. Res.* https://doi.org/10.1007/s11356-022-20023-5.
29. S. Thirumalvalavan and N. Senthilkumar, *Ind. J. Eng. Mater. Sci.* **26** (2018) 59.
30. O. A. Ogunsanya, A. A. Akinwande, O. A. Balogun, V. Romanovski and M. S. Kumar (2022), https://doi.org/10.1080/02726351.2022.2065652.
31. G. B. Mallikarjuna and E. Basavaraj, *Int. J. Sci. Eng. Res.* **12** (2021) 61.
32. P. Anand, D. Rajesh, N. Lenin, V. Balaji, V. K. B. Raja and K. Palanikumar, *Mater. Today Proc.* (2021), https://doi.org/10.1016/j.matpr.2021.01.848.
33. P. K. Bannaravuri and A. K. Birru, *Results Phys.* **10** (2018) 360. https://doi.org/j.rinp.2018.06.004.
34. A. R. K. Swamy, A. Ramesha, G. B. V. Kumar and J. N. Prakash, *J. Miner. Mater. Charact. Eng.* **10** (2011) 1141.
35. T. Sivakumar, C. Udagani, M. Sivaranjani, M. Sudhakar, R. M. Alharbi, N. Abdel-Raouf, I. B. M. Ibraheem, E. N. Sholkamy, M. A. Mahadik and S. Yishak, *Adv. Mater. Sci. Eng.* **2022** (2022) 1. https://doi.org/10.1155/2022/2286713.
36. A. A. Adediran, A A. Akinwande, O. A. Balogun, B. J. Olorunfemi and M. S. Kumar, *Sci. Rep.* **11** (2021) 19860. https://doi.org/10.1038/s41598-021-99168-1.
37. A. A. Akinwande, A. A. Adediran, O. A. Balogun, M. E. Yibowei, A. A. Barnabas, H. K. Henry and B. J. Olorunfemi, *Heliyon* **8** (2022) e09350. https://doi.org/10.1016/j.heliyon.2022.e09350.